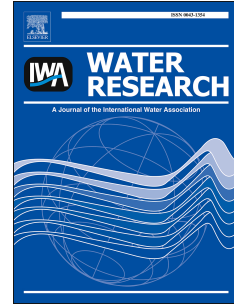


Accepted Manuscript

Impact of fluctuations in gaseous H₂S concentrations on sulfide uptake by sewer concrete: the effect of high H₂S loads

Xiaoyan Sun, Guangming Jiang, Philip L. Bond, Jurg Keller



PII: S0043-1354(15)30027-0

DOI: [10.1016/j.watres.2015.05.044](https://doi.org/10.1016/j.watres.2015.05.044)

Reference: WR 11319

To appear in: *Water Research*

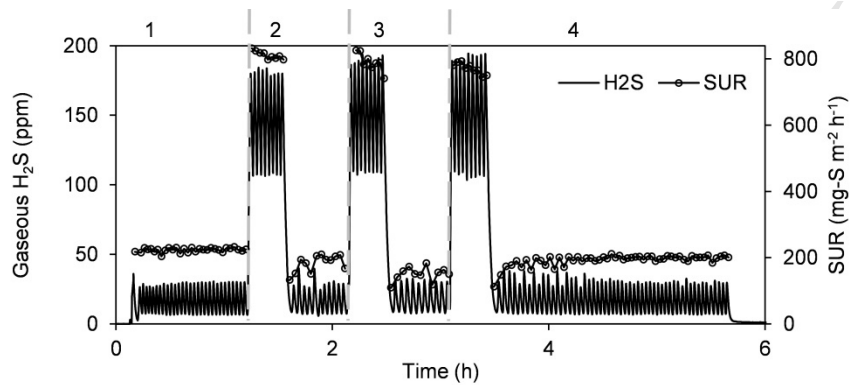
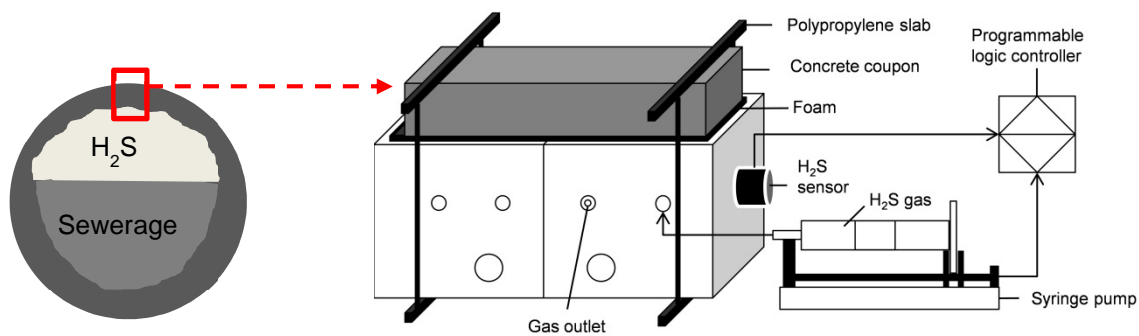
Received Date: 22 January 2015

Revised Date: 7 April 2015

Accepted Date: 22 May 2015

Please cite this article as: Sun, X., Jiang, G., Bond, P.L., Keller, J., Impact of fluctuations in gaseous H₂S concentrations on sulfide uptake by sewer concrete: the effect of high H₂S loads, *Water Research* (2015), doi: 10.1016/j.watres.2015.05.044.

This is a PDF file of an unedited manuscript that has been accepted for publication. As a service to our customers we are providing this early version of the manuscript. The manuscript will undergo copyediting, typesetting, and review of the resulting proof before it is published in its final form. Please note that during the production process errors may be discovered which could affect the content, and all legal disclaimers that apply to the journal pertain.



1 **Impact of fluctuations in gaseous H₂S concentrations on sulfide uptake by sewer**
2 **concrete: the effect of high H₂S loads**

3 Xiaoyan Sun, Guangming Jiang, Bond Philip L., Jurg Keller*

4 Advanced Water Management Centre, Gehrmann Building, Research Road, The University
5 of Queensland, St. Lucia, Queensland 4072, Australia

6 * Corresponding author. Tel.: +61 (0)7 33654727; fax: +61 (0)7 33654726.

7 Email: x.sun@awmc.uq.edu.au, g.jiang@awmc.uq.edu.au, phil.bond@awmc.uq.edu.au,
8 j.keller@awmc.uq.edu.au

9

10

11

12

13

14

15

16

17

18

19

20 **Abstract**

21 The acid production from the oxidation of hydrogen sulfide (H_2S) in sewer air results in
22 serious corrosion of exposed concrete surfaces in sewers. Large fluctuations of gaseous H_2S
23 concentrations occur in sewers due to the diurnal profiles of sewage flow and retention times
24 and the necessity of intermittent pumping of sewage from pressure pipes into gravity pipes.
25 How the high concentrations of H_2S due to these events may affect H_2S uptake and
26 subsequent corrosion by concrete sewers is largely unknown. This study determined the
27 effect of short- and long-term increases in H_2S levels on the sulfide uptake rate (SUR) of
28 concrete surfaces with an active corrosion layer. The results showed that during the high load
29 situation the SUR increased significantly but then decreased (compared to the baseline SUR)
30 by about 7 – 14% and 41 – 50% immediately after short- and long-term H_2S high-load
31 periods, respectively. For both exposure conditions, the SUR gradually (over several hours)
32 recovered to approximately 90% of the baseline SUR. Further tests suggest multiple factors
33 may contribute to the observed decrease of SUR directly after the high H_2S load. This
34 includes the temporary storage of elemental sulfur in the corrosion layer and inhibition of
35 sulfide oxidizing bacteria (SOB) due to high H_2S level and temporary acid surge.
36 Additionally, the delay of the corrosion layer to fully recover the SUR after the high H_2S load
37 suggests that there is a longer-term inhibitive effect of the high H_2S levels on the activity of
38 the SOB in the corrosion layer. Due to the observed activity reductions, concrete exposed to
39 occasional short-term high H_2S load periods had an overall lower H_2S uptake compared to
40 concrete exposed to constant H_2S levels at the same average concentration. To accurately
41 predict H_2S uptake by sewer concrete and hence the likely maximum corrosion rates, a
42 correction factor should be adopted for the H_2S fluctuations when average H_2S levels are
43 used in the prediction.

44 **Key words:** hydrogen sulfide; fluctuation; high load; sewer; concrete; corrosion

45 1. Introduction

46 Sulfide induced concrete corrosion in sewers is present worldwide, causing severe structural
47 deterioration and ultimate structural damage to wastewater catchment networks, requiring
48 very difficult and costly rehabilitation efforts (Sydney et al., 1996; US Environmental
49 Protection Agency 2010). According to ASCE's 2013 Report Card for America's
50 Infrastructure and the report from United States Environmental Protection Agency (US
51 Environmental Protection Agency 2010), many of the approximately 1.2 million km of sewer
52 mains in the United States were installed after World War II and are in need to be repaired or
53 replaced now. The sewer rehabilitation costs in US were estimated to be about \$3.2 billion
54 for 2009 alone and the national capital investment for repair of the wastewater and
55 stormwater system is evaluated to be approximately \$298 billion in the next twenty years (US
56 Environmental Protection Agency 2010). Hence protecting sewers from deterioration has a
57 major beneficial impact globally through increased service life and reduced
58 repair/replacement costs.

59 In sewers, sulfide is produced by a diverse group of bacteria (e.g. *Desulfovibrio desulfuricans*)
60 using sulfate or organic sulfur as the electron acceptor in strict anaerobic conditions, mostly
61 in sediments and biofilms occurring in fully filled (pumped) pressure pipes (Hvitved-
62 Jacobsen et al., 2013; Sharma et al., 2008). The sulfide is mainly produced in the biofilm and
63 diffuses outwards into the bulk sewage (Gutierrez et al., 2008; Parker 1951; Pomeroy and
64 Boon 1976; Satoh et al., 2009; US Environmental Protection Agency 1974). Once a gas
65 phase is present in sewers, for example in partially filled gravity pipes, at manholes or
66 pumping station wet wells, H₂S can transfer from the liquid to the gas phase. The gaseous
67 H₂S can be absorbed by the exposed, wet concrete surfaces and chemically and/or
68 biologically oxidized to sulfuric acid. Sulfide oxidizing bacteria (SOB) are detected in the
69 biofilms in aerobic (gas-phase exposed) sections of sewer pipes and their sulfuric acid

70 production is directly associated with concrete corrosion (Cayford et al., 2012; Ling et al.,
71 2014; Okabe et al., 2007; Pagaling et al., 2014). The reactions between sulfuric acid and
72 concrete components (e.g. calcium silicate hydrates) will form expansive products, e.g.
73 ettringite and gypsum, causing cracks and loss of mechanical strength of the concrete pipe
74 (Müllauer et al., 2013; O'Connell et al., 2010; Zivica and Bajza 2001). However, recent
75 findings indicate that the iron dissolution in the corrosion layer and rust precipitation near the
76 corrosion front was the actual cause for the formation of cracks, which accelerated the overall
77 corrosion process (Jiang et al., 2014b).

78 To facilitate the prediction and extension of the service-life of concrete sewers, it is very
79 important to identify the relationship between environmental factors and the concrete
80 corrosion rate. It has been recognized for decades that environmental factors, such as relative
81 humidity, temperature and H₂S levels, can affect the concrete corrosion rate (Apgar and
82 Witherspoon 2007; Islander et al., 1991; Parker 1951; Rootsey et al., 2012; Wiener et al.,
83 2006). However, research on identifying the effects of key environmental factors on concrete
84 corrosion is still limited due to the very slow progression of concrete corrosion and the
85 difficulties of measuring directly relevant factors under realistic conditions (Romanova et al.,
86 2014). In fact, many studies related to concrete corrosion were conducted through accelerated
87 experiments under conditions that are very different from those in real sewers (De Belie et al.,
88 2002; Herisson et al., 2013; Yousefi et al., 2014). Recently, laboratory studies were
89 performed over several years under controlled conditions to simulate the corrosion processes
90 in the sewer environment (Jiang et al., 2014a; Joseph et al., 2012). The results clearly
91 confirmed that H₂S is the key influencing factor determining concrete corrosion rates.
92 Additionally it was found that relative humidity was important only for the sewer crown areas
93 while temperatures between 15-30°C showed no obvious difference.

94 Well-designed laboratory investigations of sewer corrosion can mimic sewer conditions
95 (Jiang et al., 2014a; Joseph et al., 2010). However, in these laboratory-based investigations
96 the concrete is typically exposed to a constant level of H_2S , which is quite different to the
97 conditions observed in real sewers. In pressure pipes of real sewers, significant amounts of
98 sulfide can be built up during the hydraulic retention time (HRT) that typically reaches
99 several hours in such rising mains (Pomeroy and Boon 1976; Sharma et al., 2008). Sewage
100 containing high concentrations of sulfide is then periodically pumped from pressure pipes
101 into gravity pipes. The pumping events create turbulent flow conditions near the outlet of the
102 pressure pipe and in the gravity pipe downstream and thus increase the H_2S transfer from the
103 liquid phase (sewage) into the gaseous head space of the gravity pipes. This leads to sudden
104 increases of H_2S levels in the gravity pipe gas phase, creating so called 'spikes' or H_2S peak
105 concentrations. During the pump off period, the H_2S concentration in the headspace is
106 reduced due to the uptake of H_2S by concrete exposed to the gas phase and possible
107 dissolution in the continuously flowing sewage, as well as ventilation of the sewer air. These
108 effects are significantly exacerbated due to the diurnal flow variation and the corresponding
109 change in retention time in the pumped rising mains (Sharma et al., 2008). As a consequence,
110 the periodical pumping events and the temporal variation of sulfide concentrations can
111 intermittently create gaseous H_2S levels up to 100 times as high as the average concentrations,
112 most typically in the first pump cycles in the morning (Gutierrez et al., 2012; Jiang et al.,
113 2013). How this temporal variation of gaseous H_2S levels affects the sulfide uptake activity
114 of concrete with an active sulfide-induced corrosion layer is largely unknown.

115 This study investigated the effects of such H_2S peak concentrations on the sulfide uptake
116 activity of corroding concrete. The concrete utilised in this study was incubated in laboratory
117 chambers under conditions similar to those in real sewers. The influence of short- and long-
118 term high H_2S load scenarios on the sulfide (H_2S) uptake rate (SUR) was determined. Further

119 tests were carried out to examine the cumulative effect of high H₂S loads on the SUR of
120 corroding concrete and the impact of historical H₂S exposure levels on the SUR during and
121 after high H₂S loads.

122 **2. Materials and methods**

123 **2.1. H₂S profiles in real sewers**

124 Gaseous concentrations of H₂S were monitored at five minute intervals in a manhole at
125 Melbourne's Western Trunk Sewer (WTS) from 5th April 2011 to 11th April 2011 (Figure
126 S1A in Supplementary Information (SI)) and at one minute intervals in a manhole at
127 Queensland's Sunshine Coast region (Morgans discharge manhole, Unity Water, Queensland,
128 Australia) from 25th June 2014 to 1st July 2014 (Figure S1B in SI). The measured H₂S
129 concentration profiles were analysed to identify the characteristics of H₂S peak
130 concentrations, particularly the frequency and the scale of the high H₂S load events. These
131 H₂S high load events occurring in real sewers were used to design high H₂S load experiments
132 in the lab-scale system and to investigate their effect on H₂S uptake by concrete. In this study,
133 the level and duration of H₂S peak events was designed to be between five and ten times the
134 average H₂S level for a duration of 8 to 25 mins. In addition, the temperature in this study
135 was also controlled to a level similar to those observed in the real sewers, which was
136 relatively constant over the testing period with an average of 22.6 °C and 22.9 °C for
137 Melbourne and Unity Water sewers, respectively.

138 **2.2. Concrete coupons and corrosion chambers**

139 Several corrosion chambers were designed and set up to incubate concrete coupons over
140 several years under corrosive conditions. Each chamber was made of glass panels (thickness
141 4 mm) and had a length of 550 mm, width of 450 mm and height of 250 mm. The concrete
142 coupons were cut from a corroded concrete sewer pipe that was replaced after 70 years of

143 service in Sydney (Sydney Water Corporation, Australia). The dimensions of each coupon
144 were approximately 100mm (length) × 70 mm (width) × 70 mm (thickness). After cutting,
145 the coupons were washed with tap water to remove surface contaminants and dried in an
146 oven for 3 days (Joseph et al., 2010). Each coupon was partially embedded in a stainless steel
147 casing fixed by epoxy (FGI R180 epoxy & H180 hardener) with the surface that previously
148 formed the ceiling surface of the sewer pipe protruding 10 – 20 mm above the epoxy surface.
149 These coupons were then exposed to the gas phase of the corrosion chamber with the
150 exposure surface facing downwards. This arrangement of concrete coupon is to simulate the
151 position of the concrete in the crown area of real sewer pipes.

152 Three corrosion chambers were set up with three different H₂S levels (i.e. 5, 15 and 50 ppm)
153 for this study. The relative humidity and temperature of all chambers was controlled at 100%
154 and 22 – 25 °C, respectively. Each chamber contained 2.5 L of domestic sewage (collected
155 from a pumping station in Brisbane, Australia) that was replaced every 14 days. Gaseous H₂S
156 levels in the chambers were achieved and controlled by dosing Na₂S solution into a container
157 located inside the chamber and filled with HCl solution using a solenoid pump (120SP1220-
158 4TP Solenoid Operated Micro-pump, BIO-CHEM Fluidics) controlled by a programmable
159 logic controller (PLC). The chambers were arranged in drawers in a temperature controlled
160 lab (22 – 25 °C). The sewage in the chamber was warmed slightly by recirculating warm
161 water through two glass tubes submerged in it. This arrangement ensures that the relative
162 humidity in the gas phase of the chamber can be maintained at about 100% (Joseph et al.,
163 2010). The relative humidity was determined with wet and dry bulb temperatures measured
164 by resistance temperature detectors.

165 The concrete coupons were exposed to these corrosion conditions for more than 3 years to
166 establish strong corrosion activity before this study, which was indicated by the visible,
167 active corrosion layer on the surface of the coupons and the measured surface pH of all

168 coupons being below 4 (measured by surface pH probe with 4 independent measurements on
169 each coupon surface).

170 **2.3. H₂S uptake measurement system**

171 Concrete corrosion in sewers is largely driven by production of sulfuric acid through
172 oxidation of sulfide. The SUR of concrete is shown to be a good indicator to estimate the
173 maximum rate of sulfide induced concrete corrosion (Sun et al., 2014; US Environmental
174 Protection Agency 1974). In this study, the SUR by the concrete coupons was measured
175 using the method modified from that described in Sun et al., (2014) (Figure 1). To briefly
176 describe the method, we use an example to measure the SUR of a concrete coupon at 15 ppm
177 H₂S. A coupon was retrieved from the corrosion chamber and immediately placed into the
178 H₂S uptake reactor where the relative humidity was controlled at 100%. Gaseous H₂S was
179 added from a 50 mL syringe into the H₂S uptake reactor to achieve a reactor concentration of
180 20 ppm. The H₂S uptake profile of the coupon was recorded using a H₂S detector (App-Tek
181 OdaLog[®] Logger L2, detection range of 0-200 ppm). The SUR of the coupon at 15 ppm of
182 H₂S was calculated using the monitored H₂S profiles (Sun et al., 2014). To repeatedly
183 measure the SUR at 15 ppm, the addition of gaseous H₂S into the reactor was performed
184 when the monitored H₂S concentration in the reactor gas phase decreased to 10 ppm. A
185 programmable Logic Controller (PLC) was employed to monitor the H₂S concentration
186 inside the reactor and to trigger the syringe pump (NEW Era Model 501 OEM syringe pump
187 with stall detection) to add further gaseous H₂S. The PLC was used to run a pre-determined
188 sequence of low and high H₂S concentrations at a specified frequency. To avoid the build-up
189 of pressure inside the reactor during the dosing of gaseous H₂S, a small gas outlet from the
190 reactor was kept open through a needle (0.5 mm in diameter) inside a rubber stopper with a
191 non-metallic luer-lock connector on the inside of the reactor (to avoid the potential of metal
192 (needle) catalysed sulfide oxidation).

193

[INSERT FIGURE 1]

194 The background uptake rates of H₂S were determined by removing the coupon, resealing the
195 reactor with a piece of foam panel and a stainless steel sheet and repeating the H₂S injection
196 and monitoring process. The background uptake rates of the whole reactor (but without the
197 coupon) were subtracted from the measured SUR with the coupons in place to obtain the net
198 uptake rates for the concrete coupons (see Equation S1 in the Supplementary Information (SI).

199 **2.4.Batch tests**

200 **2.4.1. Effect of H₂S peak concentrations**

201 Two types of H₂S concentration high load scenarios were investigated, i.e. short- and long-
202 term. These were designed to mimic the H₂S fluctuations typically observed in real sewers.

203 The test to identify the effect of short-term high H₂S load conditions on the SUR was carried
204 out on a coupon previously exposed to 15 ppm for 53 months. Gaseous H₂S was
205 intermittently infused into the uptake reactor containing the concrete coupon. The gaseous
206 H₂S concentration in the uptake reactor was maintained between 10 and 20 ppm (averaging
207 15 ppm) for 30 mins. This simulates the historical exposure level (i.e. 15 ppm) of H₂S of the
208 coupon in the corrosion chamber. Based on the temporal H₂S uptake profiles, the SUR of the
209 coupon at 15 ppm after each injection of H₂S was calculated according to methods developed
210 previously (Sun et al., 2014). The average SUR at 15 ppm was termed the baseline SUR.
211 Then, the gaseous H₂S in the uptake reactor was quickly raised to 160 ppm and gradually
212 decreased to baseline level due to the uptake by the coupon. This intends to simulate the
213 short-term high H₂S load event. The duration of the short-term high load event was usually
214 around 7 to 8 mins. Following that, intermittent injection of H₂S at a level between 10 and 20
215 ppm was performed again. The corresponding SUR at 15 ppm was measured and compared
216 with the baseline SUR. To facilitate the comparison of the SUR prior to and after a high H₂S

217 load, the relative SUR ratio, defined as the SUR divided by the baseline SUR, was calculated.
218 The experiment with H₂S concentration up to 160 ppm was repeated three times. The SUR
219 after each high loading event was calculated and compared with the baseline SUR.

220 To investigate the influence of the long-term high load of H₂S concentrations on the SUR,
221 one uptake test was carried out on the same coupon after 54 months of corrosion chamber
222 exposure with a similar test procedure. The only difference was that the duration of the high
223 H₂S level was maintained for 20 to 22 mins, which was achieved through intermittent
224 injection of gaseous H₂S to keep the H₂S level between 115 and 160 ppm. The corresponding
225 SUR at 130 ppm was calculated using the monitored H₂S uptake profiles. A control test was
226 carried out on the same coupon through intermittently injecting H₂S to around 10 and 20 ppm
227 for 3 h.

228 **2.4.2. Cumulative inhibition effect of high H₂S load**

229 The post-exposure inhibition effect of high H₂S concentrations on the SUR of the concrete
230 coupon was determined using a coupon previously exposed to 15 ppm H₂S for 42 months in
231 the corrosion chamber. The experiment included two independent H₂S uptake tests with
232 different H₂S exposure profiles but the same average H₂S exposure level.

233 For the first test, to simulate the historical H₂S exposure level (i.e. 15 ppm) of the coupon in
234 the corrosion chamber, gaseous H₂S was intermittently injected into the uptake reactor to
235 maintain the gaseous H₂S level in the uptake reactor between 10 and 20 ppm for 110 min.
236 The corresponding SUR at 15 ppm after each injection of H₂S was calculated and termed as
237 the baseline SUR. Then, the coupon was exposed to various high loads of H₂S , i.e. H₂S
238 levels between 160 and 180 ppm for about 45 min, between 110 and 130 ppm for about 45
239 min and between 65 and 85 for about 45 min. The corresponding relative SUR ratio was

240 calculated by dividing the experimental SUR by the baseline SUR, for each high loading
241 event.

242 The second test was carried out in a similar procedure but the exposure H₂S profiles were
243 different. Following the baseline exposure between 10 to 20 ppm H₂S, the coupon was
244 exposed to different, and increasing H₂S levels for 45 minutes in each experiment, namely at
245 65 to 85 ppm, 110 to 130 ppm and 160 to 180 ppm H₂S. The corresponding relative SUR
246 ratio for each experiment was calculated as described above.

247 The duplicate experiment was conducted on a coupon previously exposed to 15 ppm H₂S for
248 38 months in the corrosion chamber.

249 **2.4.3. The effect of H₂S spikes on coupons with different exposure histories**

250 To examine the effect of the high-level H₂S exposure on coupons that had previously been
251 maintained at different H₂S levels, three coupons previously exposed to either 5, 15 and 50
252 ppm were tested. To examine the effect of various H₂S spike scenarios on the overall amount
253 of H₂S taken up, several tests (shown in Table 1) were carried out to compare the amount of
254 H₂S uptake by each coupon at its historical H₂S level (i.e. 'control' test) and various H₂S
255 spike situations (i.e. 'spike' test) over the same exposure time.

256 [INSERT TABLE 1]

257 Over the experimental period of a specific 'spike' test, the mass of H₂S taken up by the
258 concrete coupon surface is termed T_{spike} ((mg-S), see details of calculation in Equation S2 in
259 SI). Over a duration equivalent to that of the specific 'spike' test, the mass of H₂S taken up by
260 the same coupon surface when exposed to the baseline H₂S concentration is termed T_{baseline}
261 ((mg-S), see details of calculation in Equation S4 in SI).

262 Therefore, the ratio (α) is defined for a specific coupon by the mass of H₂S taken up by the
263 concrete coupon in a 'spike' test compared to the uptake by the same concrete coupon when
264 exposed to a constant H₂S level (i.e. historical exposure level) over the same time:

$$265 \quad \alpha = \frac{T_{\text{spike}}}{T_{\text{baseline}}} \quad (1)$$

266 **3. Results and discussion**

267 **3.1. Effect of high H₂S load**

268 **3.1.1. Short-term high load of H₂S**

269 Figure 2A shows the temporal H₂S uptake profiles of a concrete coupon over 3 h and the
270 corresponding SUR measured after each injection of gaseous H₂S. At stage 1, the repeated
271 measurement of SUR of the coupon at its historical exposure level of H₂S (i.e. 15 ppm) was
272 relatively constant, averaging 173 mg-S m⁻² h⁻¹. Similarly, Figure S2 in SI shows the stability
273 of the SUR during a control experiment, expressed as percentage relative to the baseline SUR.
274 This suggests that the SUR of a specific coupon will be quite constant when the H₂S exposure
275 level is constant. However, immediately after experiencing the first H₂S peak concentration
276 (stage 2), the SUR of the coupon at 15 ppm decreased to 149 mg-S m⁻² h⁻¹, which was about
277 14% lower than the baseline SUR (Figure 2B). Following that, the SUR rose gradually to 96%
278 of baseline SUR over about 10-20 minutes. Compared to stage 2, the decrease of SUR after
279 the second (stage 3) and third (stage 4) H₂S peak concentration is similar, but the recovery is
280 less. Especially, no recovery of SUR was observed within about 1 h after the third peak. It
281 seems that there was a temporary inhibition initially, which then became more persistent.

282 [INSERT FIGURE 2]

283 The immediate decrease of SUR after the high H₂S load could be explained as follows.
284 Elemental sulfur (S⁰) would likely be produced as intermediate product during sulfide

285 oxidation (Jensen et al., 2009; Nielsen et al., 2014). Part of this S^0 may be directly oxidized to
286 sulfate and hence would compete with sulfide as electron donors for SOB. Another part of
287 this may remain as an intermediate and undergo a slower oxidation process (Jensen et al.,
288 2009; Nielsen et al., 2014). During the high load period, increased amount of S^0 may be
289 produced and stored temporarily in the corrosion layer. Immediately after the high H_2S load,
290 part of the S^0 was further oxidized which could consequently reduce the SUR temporarily.
291 With the ongoing oxidation of S^0 in the corrosion layer after the H_2S loading, the previously
292 accumulated S^0 would be gradually consumed, and the SUR would recover. Under some
293 circumstances, such as after the quick reduction of H_2S peak concentrations by sewer
294 ventilation, some H_2S accumulated in the corrosion layer during the previous high load
295 periods may even diffuse back into the gas phase, resulting in a negative SUR (see details in
296 Table S1 in the SI)).

297 However, the diminishing recovery capacity of the SUR after several high H_2S loading
298 experiments suggests a possible inhibitive effect of this loading on the SOB activity. The
299 probable inhibition of SOB by high sulfide loads has also been reported in sewer concrete
300 corrosion layers that were periodically exposed to 1000 ppm_v of H_2S and loadings of up to
301 340 mg-S m⁻² h⁻¹ (Nielsen et al., 2014). In other studies, the inhibitory effect of high sulfide
302 loads onto biological sulfide oxidation activity was detected to occur in denitrifying and
303 sulfide oxidizing conditions (Buisman et al., 1990; Buisman et al., 1991; Cardoso et al., 2006;
304 Mahmood et al., 2008; Wirsén et al., 2002). A possible explanation for this effect could be
305 that the temporary increase in sulfide and hence sulfuric acid formation reduces the pH within
306 the biofilm/corrosion layer temporarily until this is neutralized by the corroding concrete
307 again over time. Further detailed investigations may be necessary to corroborate this
308 hypothetical explanation.

309 **3.1.2. Long-term high load of H_2S**

310 Figure 3A (stage 1) shows that the baseline SUR of the coupon prior to the high load
311 experiments was around $225 \text{ mg-S m}^{-2} \text{ h}^{-1}$ and hence slightly higher than that in the previous
312 test shown in Figure 2A. This difference of the absolute SUR value for the same coupon
313 within about 1 month may be due to various effects, possibly related to the absorbed moisture
314 in the corrosion biofilm. As this study is aimed at identifying the immediate changes of SUR
315 caused by high H_2S load, such variations of the absolute SUR have a negligible impact on the
316 results.

317 [INSERT FIGURE 3]

318 Upon long-term exposure to high levels of H_2S (Figure 3A, stage 2), the SUR of the coupon
319 at 15 ppm H_2S immediately decreased by 41%. The SUR gradually recovered to
320 approximately 86% - 92% of the baseline SUR during the following the following 6 – 15
321 minutes. The observed decreases of the SUR after the 2nd and 3rd long-term high-level
322 exposure (stage 3 & 4) were even slightly larger than that after the 1st long-term exposure and
323 the recovery of the SUR was also slower. Particularly, the final recovery level at stage 4
324 reached only 87% and 93 % 2h after the end of the high loading, indicating there is some
325 more persistent inhibition, as also observed in the short-term experiments. In addition, during
326 exposure to high H_2S levels, the coupon had a gradual decrease of the SUR at 130 ppm not
327 only within each of the three stages (stage 2, 3 and 4 in Figure 3A) but also from stage 2 to
328 stage 4.

329 Compared to the effects after the short-term exposure to high H_2S levels, the SUR clearly
330 showed a more significant decrease immediately after the long-term high H_2S load and had a
331 similar extent of recovery although the time required for the recovery of the SUR to a steady
332 level is slightly longer. Consequently, it supports that the longer-term exposure of the coupon
333 to high H_2S levels may result in a greater accumulation of S^0 in the corrosion layer, thus

334 causing a bigger decrease of the SUR after the exposure. In addition, the similar extent of
335 recovery of SUR after short- and long- term high load of H₂S suggests that the
336 duration/length of coupon exposure to high levels of H₂S may affect the rate of the SUR
337 recovery but not the extent of the recovery. This indicates that the activity of the SOB may be
338 inhibited for various lengths depending on the duration of high H₂S load.

339 **3.2. Cumulative inhibitive effect of high H₂S loads**

340 Based on the hypothetical accumulation of S⁰ in the corrosion layer discussed above, it would
341 be expected that all prior H₂S loads can have a cumulative effect on the SUR of the concrete
342 coupon unless the recovery time between high load events is sufficient to eliminate the
343 temporarily accumulated elemental sulfur. This was indeed demonstrated in a separate
344 experiment. Figures 4A&B show the results of two tests where the coupon is exposed to
345 various high H₂S load sequences but with the average H₂S concentration of the two tests
346 being similar. In Figure 4A, after exposing the concrete coupon to the baseline H₂S level
347 (stage 1), the relative SUR at 170 ppm from the 1st to the last measurement decreased by
348 about 32% (stage 2) and then the relative SUR was stable during the repeated measurement at
349 both 120 (stage 3) and 70 ppm (stage 4). The relative SUR values of the last measurements at
350 70 ppm H₂S (stage 4), 120 ppm (stage 3) and 170 ppm (stage 1) were 168%, 199% and 238%,
351 respectively. In contrast, Figure 4B shows a gradual decrease of relative SUR during the
352 repeated measurement at 70 ppm (stage 2), 120 ppm (stage 3) and 170 ppm (stage 4) and the
353 relative SUR of the last measurements at stages 2, 3 and 4 were 187%, 210% and 232%,
354 respectively.

355 [INSERT FIGURE 4]

356 The results demonstrate that an abrupt increase of the H₂S level led to gradual decrease of
357 SUR at the elevated H₂S level whereas an abrupt decrease of H₂S resulted to gradual increase

358 of SUR at the lowered H_2S level. This suggests that during the periods of high load of H_2S
359 various factors, including the storage of S^0 in the corrosion layer and the inhibition of SOB
360 activity due to high H_2S and/or temporary acid surge, may cause the observed gradual
361 decrease of SUR, which is consistent with the results and explanations given in the above
362 sections. The SUR recovery observed after the high load periods could be explained by the
363 gradual consumption of the previously accumulated S^0 and the reduced inhibition of SOB due
364 to the lower H_2S level and/or the neutralisation of acid by alkaline concrete components.
365 Compared to the trend of SUR at stage 2 in Figure 4A, the decrease of SUR at stage 2, 3 and
366 4 in Figure 4B is much less prominent, indicating that the greater the change of the H_2S levels,
367 the more obvious the change of the SUR at the new higher H_2S level seems to be.

368 In addition, the relative SUR at both 70 and 120 ppm in Figure 4A were much lower than
369 those shown in Figure 4B (summarized in Figure 4C). Therefore, it is reasonable to speculate
370 that the previous very high load of the coupon with H_2S at stage 2 (Figure 4A) has
371 significantly inhibited the biological sulfide oxidation activity for some extended period
372 (hours), which is also supported by the results shown in the previous sections. Similar
373 phenomena were also observed in a repeat experiment on a pre-corroded coupon with a much
374 higher absolute SUR than the one shown here (Figure S3 in SI).

375 **3.3. Effects of high H_2S loads on coupons with different exposure history**

376 The effects of the high H_2S concentrations on coupons with different H_2S historic exposure
377 levels were compared. Figure 5 shows the values of α (as defined in Equation 4) plotted
378 against the high H_2S level in each uptake test. For all the three coupons, the values of α
379 increased with the increase of the high H_2S load level although the incremental increases of α
380 were smallest and largest for the coupons previously exposed to 50 and 5 ppm of H_2S ,
381 respectively. This indicates that the value of α and the historical exposure level of H_2S of

382 concrete coupons are inversely correlated, partly due to that the baseline SUR is much lower
383 for 5 ppm coupon compared to 50 ppm coupon. In addition, it suggests that the lower the
384 historical exposure level of H₂S, the more sensitive the H₂S uptake of the coupon is towards a
385 high H₂S load. This is reasonable as the SOB adapted to continuously higher levels of H₂S
386 have a much higher activity and therefore are less susceptible to the occasional peak levels of
387 H₂S.

388 [INSERT FIGURE 5]

389 Interestingly, the values of α were below 1 for all coupons when the high levels of H₂S were
390 around 1.5 to 2 times of the baseline H₂S levels. This suggests that during the exposure to
391 modest H₂S loads the coupons may actually have a lower H₂S uptake rate compared to that
392 under constant H₂S baseline conditions. Extrapolating this finding to a specific section of real
393 sewer pipe with active corrosion layers, it would suggest that the occurrence of relative low
394 H₂S peak levels due to short-term pumping events may not cause any additional H₂S uptake,
395 but may even result in a slightly lower level of H₂S uptake compared to a situation with a
396 steady H₂S level having the same average H₂S concentration. On the contrary, having periods
397 with high H₂S loads when the baseline levels are low (e.g. 5 ppm), will result in the highest
398 levels of sulfide uptake amounts. Therefore, these conditions with extremely high H₂S levels
399 should be avoided to minimize H₂S flux and thus corrosion activity and prolong sewer life.

400 **3.4. Implications**

401 This study reveals that the presence of occasional high H₂S levels in sewer atmosphere has an
402 inhibitory effect on H₂S uptake by sewer concrete. Estimating the H₂S uptake simply based
403 on the *average* H₂S level will therefore cause an overestimation of the H₂S uptake and hence
404 the corresponding corrosion rate if there are significant fluctuations in the gas phase H₂S
405 concentrations, which is commonly the case. For example, calculating the mass of H₂S taken

406 up by a concrete pipe over 24 h based on the SUR at the *average* H₂S concentration may lead
407 to an overestimation of the H₂S uptake compared to an integration of the *actual* SUR over
408 time. It is due to the following two reasons. First, the SUR follows a nth order relative to the
409 H₂S concentration with n being below 1 (Sun et al., 2014; Vollertsen et al., 2008), which
410 indicates that the average SUR over the 24 h is smaller than the SUR at the average H₂S
411 concentration. Second, the actual average SUR is smaller than the average SUR over 24 h
412 due to the fact that the SUR at low H₂S levels is affected by the inhibition effect from
413 preceding high H₂S load events.

414 The total sulfide uptake by a concrete surface over seven days exposed to Sydney sewers
415 calculated based on the real H₂S profile and the average H₂S level (i.e. 5.2 ppm) was 722 and
416 766 mg-S m⁻² respectively, suggesting that the calculation from the average H₂S level
417 resulted to an overestimation of at least 5.8%. Therefore, a correction factor will need to be
418 implemented when calculating the H₂S uptake based on SUR at average H₂S level. However,
419 since the reduction in SUR will directly depend on the actual high H₂S load profile and the
420 exposure history of the concrete, the correction factor will need to be determined on a case-
421 by-case basis using the actual or expected H₂S profiles.

422 **4. Conclusions**

423 This study examined the behaviour of H₂S uptake by concrete under various high H₂S load
424 scenarios. The main findings from this work are:

- 425 • Both short and long high H₂S load events decrease the SUR of concrete coupons. The
426 latter leads to a larger temporary reduction of SUR whereas they cause similar
427 persistent inhibition effects.

- 428 • Sequential exposures to elevated H₂S levels create a cumulative effect on the SUR,
429 which is more pronounced if there is a rapid initial increase rather than a gradual
430 increase in H₂S.
- 431 • The sensitivity of the H₂S uptake rate by the corrosion layer towards high H₂S loads is
432 largely dependent on the historical H₂S exposure levels. Large H₂S loads on a low
433 baseline concentration have a more pronounced impact on the total sulfide uptake
434 than modest increases on top of higher H₂S levels. However, it has to be considered
435 that for a specific, actively corroding concrete surface higher average H₂S
436 concentrations always create more corrosive conditions than lower levels.
- 437 • Due to the rapid decrease and slow recovery effect of H₂S spikes on the SUR, an
438 estimation of the corrosion effect purely on the average H₂S concentrations may result
439 in an overestimation of the total H₂S uptake and thus probably an overestimation of
440 the concrete corrosion rates.

441 **5. Acknowledgments**

442 This study was supported by the Australia Research Council and many partners from the
443 Australian water industry (Sewer Corrosion and Odour Research Project LP0882016). The
444 PhD student Xiaoyan Sun would like to acknowledge The University of Queensland for the
445 provision of a Tuition Fee International Scholarship and the Chinese Scholarship Council for
446 the Living Allowance Scholarship. Dr Guangming Jiang is the recipient of a Queensland
447 State Government's Early Career Accelerate Fellowship.

448 **6. References**

449 Apgar, D. and Witherspoon, J. 2007. Minimization of odors and corrosion in collection
450 systems: Phase I, Water Environment Research Foundation, Alexandria, VA, USA.

- 451 Buisman, C., Uspeert, P., Janssen, A. and Lettinga, G., 1990. Kinetics of chemical and
452 biological sulphide oxidation in aqueous solutions. *Water research (Oxford)*. 24 (5), 667-671.
- 453 Buisman, C.J.N., Jspeert, P.I., Hof, A., Janssen, A.J.H., Hagen, R.T. and Lettinga, G., 1991.
454 Kinetic parameters of a mixed culture oxidizing sulfide and sulfur with oxygen.
455 *Biotechnology and bioengineering*. 38 (8), 813-820.
- 456 Cardoso, R.B., Sierra-Alvarez, R., Rowlette, P., Flores, E.R., Gómez, J. and Field, J.A., 2006.
457 Sulfide oxidation under chemolithoautotrophic denitrifying conditions. *Biotechnology and*
458 *Bioengineering*. 95 (6), 1148-1157.
- 459 Cayford, B.I., Dennis, P.G., Keller, J., Tyson, G.W. and Bond, P.L., 2012. High-throughput
460 amplicon sequencing reveals distinct communities within a corroding concrete sewer system.
461 *Applied and Environmental Microbiology*. 78 (19), 7160-7162.
- 462 De Belie, N., Monteny, J. and Taerwe, L., 2002. Apparatus for accelerated degradation
463 testing of concrete specimens. *Materials and Structures*. 35 (7), 427-433.
- 464 Gutierrez, O., Mohanakrishnan, J., Sharma, K.R., Meyer, R.L., Keller, J. and Yuan, Z., 2008.
465 Evaluation of oxygen injection as a means of controlling sulfide production in a sewer system.
466 *Water Research*. 42 (17), 4549-4561.
- 467 Gutierrez, O., Sharma, K.R. and Poch, M., 2012. Advanced assessment of sulfide and
468 methane emissions from sewers of Mediterranean cities. *International Water Association*
469 *Ecotechnologies for Wastewater Treatment ECO-STP*, 25-27 June, 2012, Santiago de
470 Compostela, Spain. Santiago de Compostela, Spain.
- 471 Herisson, J., van Hullebusch, E.D., Moletta-Denat, M., Taquet, P. and Chaussadent, T., 2013.
472 Toward an accelerated biodeterioration test to understand the behavior of Portland and
473 calcium aluminate cementitious materials in sewer networks. *International Biodeterioration &*
474 *Biodegradation*. 84, 236-243.

- 475 Hvitved-Jacobsen, T., Vollertsen, J. and Nielson, A.R.H. 2013. Sewer processes: microbial
476 and chemical process engineering of sewer networks, CRC Press, Boca Raton London New
477 York Washington, D.C.
- 478 Islander, R.L., Deviny, J.S., Mansfeld, F., Postyn, A. and Shih, H., 1991. Microbial ecology
479 of crown corrosion in sewers. *Journal of Environmental Engineering*. 117 (6), 751-770.
- 480 Jensen, H.S., Nielsen, A.H., Hvitved-Jacobsen, T. and Vollertsen, J., 2009. Modeling of
481 hydrogen sulfide oxidation in concrete corrosion products from sewer pipes. *Water*
482 *Environment Research*. 81 (4), 365-373.
- 483 Jiang, G., Keating, A., Corrie, S., O'Halloran, K., Nguyen, L. and Yuan, Z., 2013. Dosing
484 free nitrous acid for sulfide control in sewers: Results of field trials in Australia. *Water*
485 *Research*. 47 (13), 4331-4339.
- 486 Jiang, G., Keller, J. and Bond, P.L., 2014a. Determining the long-term effects of H₂S
487 concentration, relative humidity and air temperature on concrete sewer corrosion. *Water*
488 *Research*. 65, 157-169.
- 489 Jiang, G., Wightman, E., Donose, B.C., Yuan, Z., Bond, P.L. and Keller, J., 2014b. The role
490 of iron in sulfide induced corrosion of sewer concrete. *Water Research*. 49, 166-174.
- 491 Joseph, A.P., Keller, J. and Bond, P.L., 2010. Examination of concrete corrosion using a
492 laboratory experimental set up simulating sewer conditions. 6th international conference on
493 sewer processes and networks. Surfers Paradise, Gold Coast, Australia.
- 494 Joseph, A.P., Keller, J., Bustamante, H. and Bond, P.L., 2012. Surface neutralization and H₂S
495 oxidation at early stages of sewer corrosion: Influence of temperature, relative humidity and
496 H₂S concentration. *Water Research*. 46 (13), 4235-4245.
- 497 Ling, A.L., Robertson, C.E., Harris, J.K., Frank, D.N., Kotter, C.V., Stevens, M.J., Pace, N.
498 and Hernandez, M.T., 2014. Carbon dioxide and hydrogen sulfide associations with regional

- 499 bacterial diversity patterns in microbially induced concrete corrosion. *Environmental Science*
500 & *Technology*. 48 (13), 7357-7364.
- 501 Mahmood, Q., Zheng, P., Hayat, Y., Islam, E., Wu, D. and Ren-cun, J., 2008. Effect of pH on
502 anoxic sulfide oxidizing reactor performance. *Bioresource Technology*. 99 (8), 3291-3296.
- 503 Müllauer, W., Beddoe, R.E. and Heinz, D., 2013. Sulfate attack expansion mechanisms.
504 *Cement and Concrete Research*. 52, 208-215.
- 505 Nielsen, A.H., Hvitved-Jacobsen, T., Jensen, H.S. and Vollertsen, J., 2014. Experimental
506 evaluation of the stoichiometry of sulfide-related concrete sewer corrosion. *Journal of*
507 *Environmental Engineering*. 140 (2).
- 508 O'Connell, M., McNally, C. and Richardson, M.G., 2010. Biochemical attack on concrete in
509 wastewater applications: A state of the art review. *Cement and Concrete Composites*. 32 (7),
510 479-485.
- 511 Okabe, S., Odagiri, M., Ito, T. and Satoh, H., 2007. Succession of sulfur-oxidizing bacteria in
512 the microbial community on corroding concrete in sewer systems. *Applied and*
513 *Environmental Microbiology*. 73 (3), 971-980.
- 514 Pagaling, E., Yang, K. and Yan, T., 2014. Pyrosequencing reveals correlations between
515 extremely acidophilic bacterial communities with hydrogen sulphide concentrations, pH and
516 inert polymer coatings at concrete sewer crown surfaces. *Journal of Applied Microbiology*.
517 117 (1), 50-64.
- 518 Parker, C.D., 1951. *Mechanics of Corrosion of Concrete Sewers by Hydrogen Sulfide*.
519 *Sewage and Industrial Wastes*. 23 (12), 1477-1485.
- 520 Pomeroy, R.D. and Boon, A.G. 1976. *The problem of hydrogen sulfide in sewers*, London:
521 Clay Pipe Development Association.

- 522 Romanova, A., Mahmoodian, M. and Alani, M.A., 2014. Influence and interaction of
523 temperature, H₂S and pH on concrete sewer pipe corrosion. *International Journal of Civil,*
524 *Architectural, Structural and Construction Engineering.* 8 (6).
- 525 Rootsey, R., Melchers, R., Stuetz, R., Keller, J. and Yuan, Z. 2012. Taking control of odours
526 and corrosion in sewers, Australian Water Association, Sydney, Australia.
- 527 Satoh, H., Odagiri, M., Ito, T. and Okabe, S., 2009. Microbial community structures and in
528 situ sulfate-reducing and sulfur-oxidizing activities in biofilms developed on mortar
529 specimens in a corroded sewer system. *Water Research.* 43 (18), 4729-4739.
- 530 Sharma, K.R., Yuan, Z., de Haas, D., Hamilton, G., Corrie, S. and Keller, J., 2008. Dynamics
531 and dynamic modelling of H₂S production in sewer systems. *Water Research.* 42 (10–11),
532 2527-2538.
- 533 Sun, X., Jiang, G., Bond, P.L., Wells, T. and Keller, J., 2014. A rapid, non-destructive
534 methodology to monitor activity of sulfide-induced corrosion of concrete based on H₂S
535 uptake rate. *Water Research.* 59, 229-238.
- 536 Sydney, R., Esfandi, E. and Surapaneni, S., 1996. Control concrete sewer corrosion via the
537 crown spray process. *Water Environment Research.* 68 (3), 338-347.
- 538 US Environmental Protection Agency 1974. Process design manual for sulfide control in
539 sanitary sewerage systems, US Environmental Protection Agency Technology Transfer
540 Office, Washington, DC EPA-625/1-74-005.
- 541 US Environmental Protection Agency 2010. State of technology for rehabilitation of
542 wastewater collection systems, US Environmental Protection Agency, Office of Research and
543 Development. EPA/600/R-10/078, July 2010.
- 544 Vollertsen, J., Nielsen, A.H., Jensen, H.S., Wium-Andersen, T. and Hvitved-Jacobsen, T.,
545 2008. Corrosion of concrete sewers - The kinetics of hydrogen sulfide oxidation. *Science of*
546 *the Total Environment.* 394 (1), 162-170.

547 Wiener, M.S., Salas, B.V., Quintero-Núñez, M. and Zlatev, R., 2006. Effect of H₂S on
548 corrosion in polluted waters: a review. *Corrosion Engineering, Science and Technology*. 41
549 (3), 221-227.

550 Wirsen, C.O., Sievert, S.M., Cavanaugh, C.M., Molyneaux, S.J., Ahmad, A., Taylor, L.,
551 DeLong, E.F. and Taylor, C.D., 2002. Characterization of an autotrophic sulfide-oxidizing
552 marine *Arcobacter* sp. that produces filamentous sulfur. *Applied and Environmental*
553 *Microbiology*. 68 (1), 316-325.

554 Yousefi, A., Allahverdi, A. and Hejazi, P., 2014. Accelerated biodegradation of cured cement
555 paste by *Thiobacillus* species under simulation condition. *International Biodeterioration &*
556 *Biodegradation*. 86, 317-326.

557 Zivica, V.r. and Bajza, A., 2001. Acidic attack of cement based materials - a review. Part 1.
558 Principle of acidic attack. *Construction and Building Materials*. 15 (8), 331-340.

559

560

Table 1 – Details of three series of H₂S uptake tests performed on three concrete coupons with different historical exposure conditions.

Test serie	Coupon exposure history	Batch tests	H ₂ S levels (ppm)
1	5 ppm, 22-25°C, 100% RH, 39 months	Control	5
		Spike 1	10 to 5
		Spike 2	15 to 5
		Spike 3	20 to 5
		Spike 4	25 to 5
		Spike 5	50 to 5
		Spike 6	100 to 5
		Spike 7	150 to 5
2	15 ppm, 22-25°C, 100% RH, 39 months	Control	15
		Spike 1	25 to 15
		Spike 2	50 to 15
		Spike 3	75 to 15
		Spike 4	100 to 15
		Spike 5	150 to 15
3	50 ppm, 22-25°C, 100% RH, 39 months	Control	50
		Spike 1	75 to 50
		Spike 2	100 to 50
		Spike 3	125 to 50
		Spike 4	180 to 50

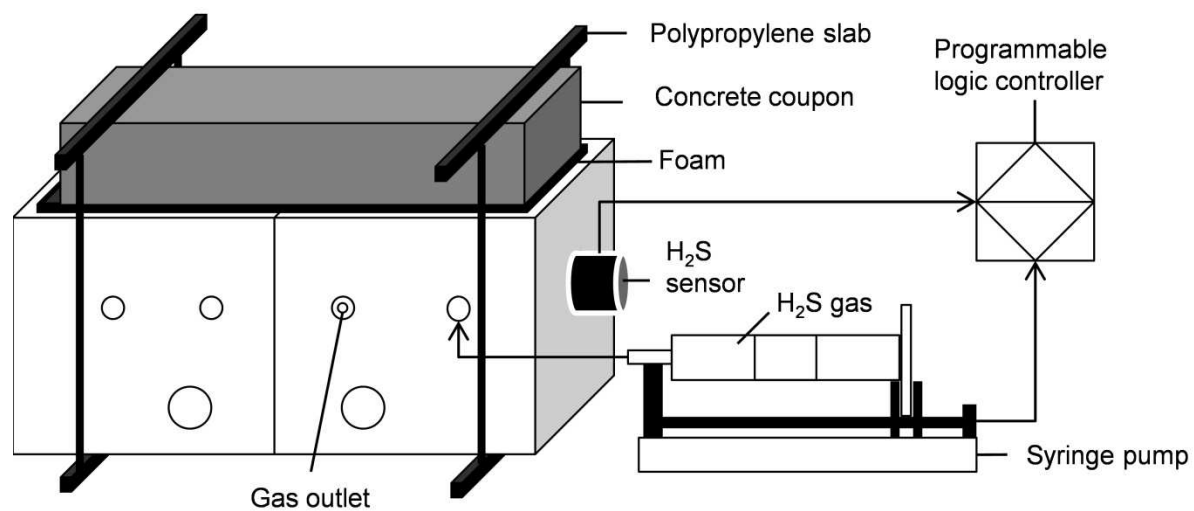


Figure – 1 The schematic diagram of the system used to measure the H₂S uptake by concrete coupons.

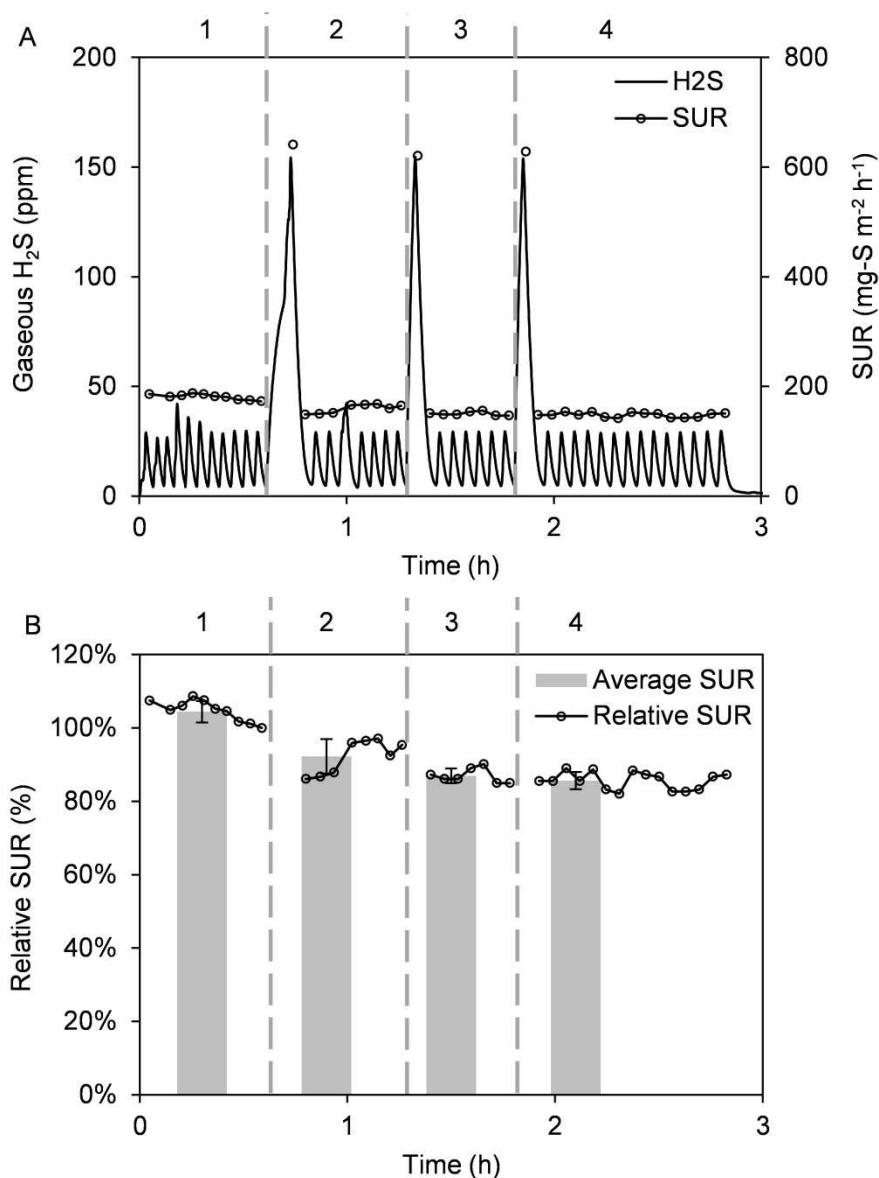


Figure 2 – The temporal H₂S uptake profiles of a coupon (exposure history: 15 ppm H₂S, 22-25 °C, 100% relative humidity for 53 months) and the corresponding SUR at the historical exposure level (i.e. 15 ppm) and peak levels (i.e. 130 ppm) of H₂S are shown in Figure A and the relative SUR and average SUR at various stages shown in Figure B. Different experimental stages (1 to 4) are listed above the plotted data in Figures A and B and the error bars in Figure B represent standard deviations.

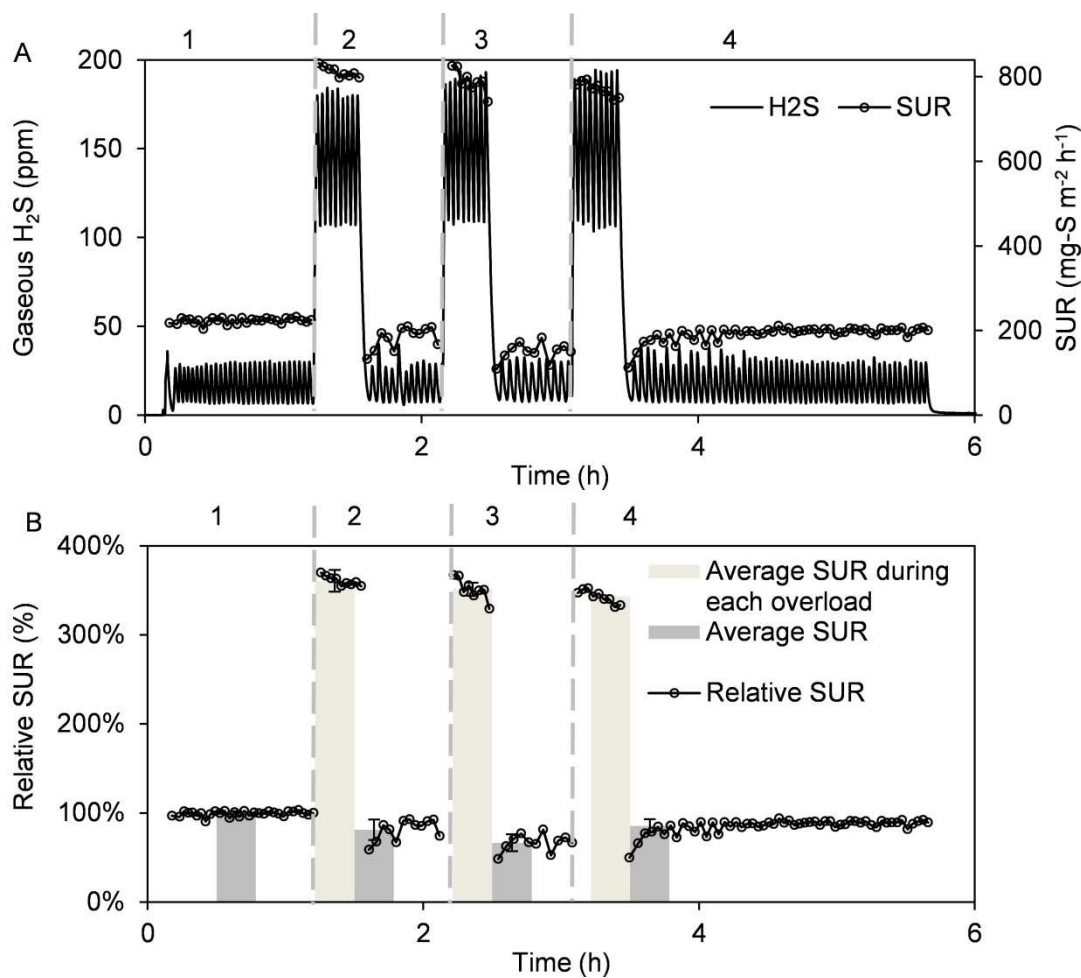


Figure 3 – The H₂S uptake profiles of the coupon (exposure history: 15 ppm H₂S, 22-25 °C, 100% relative humidity for 54 months), the corresponding SUR at its baseline H₂S level (i.e. 15 ppm) and high H₂S levels (i.e. 130 ppm) are shown Figure A and the relative SUR and the average relative SUR at each stage is shown in Figure B. Different experimental stages (1 to 4) are listed above the plotted data in Figures A and B and the error bars in Figure B represent standard deviations.

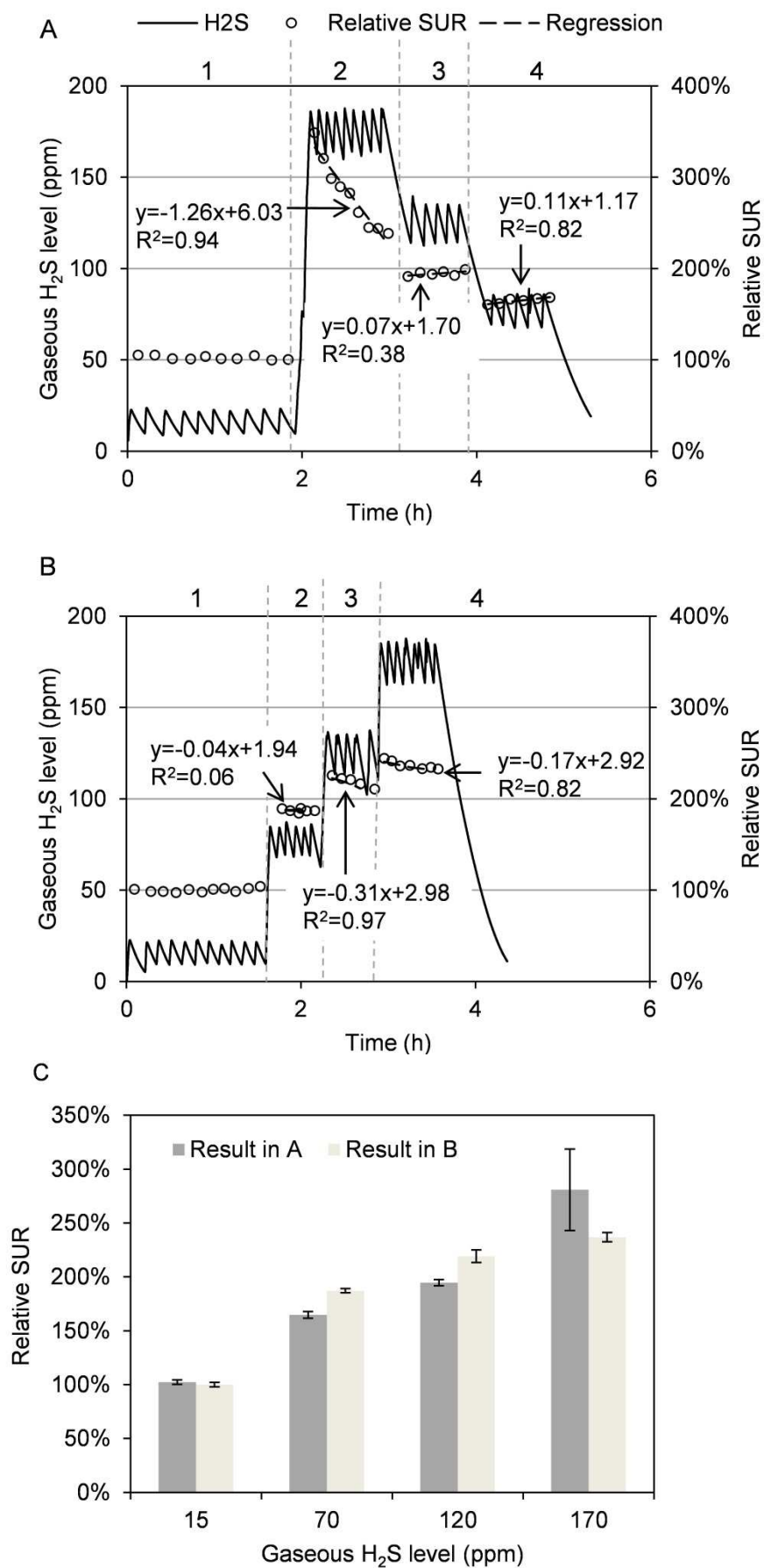


Figure 4 – The H₂S uptake profiles of a coupon (previously exposed to 15 ppm, 100% relative humidity and 22-25°C for 42 months) in a H₂S uptake test with various high loads of H₂S and the corresponding relative SUR at 15, 70, 120 and 170 ppm were shown in Figure A. The H₂S uptake profiles of the same coupon in the other test and the corresponding relative SUR was shown in Figure B. The corresponding relative SUR in Figure A and B against H₂S concentration is shown in Figure C. Different stages of the experiment are listed (1 to 4) above the plotted data on Figure A and B and the linear regression of relative SUR at each stage shown in Figure A and B was also described by the equation aside. The error bars in Figure C represent standard deviations.

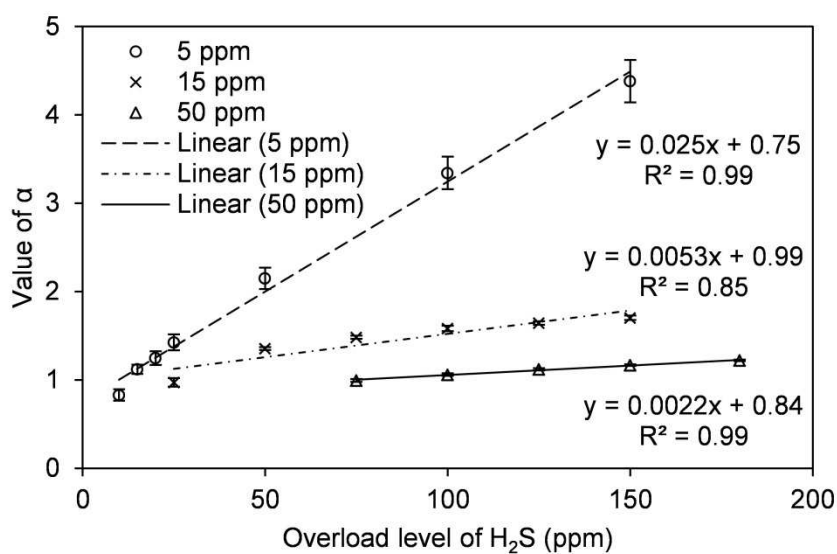


Figure 5 – The α values (dot) of coupons previously exposed to 5, 15 and 50 ppm of H₂S in corrosion chamber for 39 months were plotted against the high level of H₂S in each uptake test. Each line shows the linear regression based on the α values of each coupon and was also described by the equation aside.

Highlights:

- Gaseous H₂S concentration fluctuations in real sewers were detected and analysed
- High H₂S loads affected the H₂S uptake activity of concrete coupon
- The effect associates strongly with the duration and the scale of H₂S load
- The effect correlates with the concrete historical H₂S exposure concentrations
- Our results may facilitate better estimation of the sewer corrosion activity

1 Supplementary Information for

2 **Impact of fluctuations in gaseous H₂S concentrations on sulfide uptake by sewer**
3 **concrete: the effect of high H₂S loads**

4 Xiaoyan Sun, Guangming Jiang, Bond Philip L., Jurg Keller*

5 Advanced Water Management Centre, Gehrman Building, Research Road, The University
6 of Queensland, St. Lucia, Queensland 4072, Australia

7 * Corresponding author. Tel.: +61 (0)7 33654727; fax: +61 (0)7 33654726.

8 Email: x.sun@awmc.uq.edu.au, g.jiang@awmc.uq.edu.au, phil.bond@awmc.uq.edu.au,
9 j.keller@awmc.uq.edu.au

10

11

12

13

14

15

16

17

18

19

20 The background SUR follows first order ($R^2=0.9998$) towards the gaseous H_2S concentration
 21 (also shown in the previous study (Sun et al., 2014)) and can be expressed as:

$$22 \quad r_{H_2S,background} = k * [H_2S] = a * [H_2S] * 101.325 \text{KPa} * \frac{32 \text{g/mol}}{RT} * \frac{V}{S} \quad (\text{S1})$$

23 $r_{H_2S,background}$ is background SUR ($\text{mg-S m}^{-2} \text{h}^{-1}$), k is rate constant ($\text{mg-S m}^{-2} \text{h}^{-1} \text{ppm}^{-1}$, k
 24 was found to be $0.13 \text{mg-S m}^{-2} \text{h}^{-1} \text{ppm}^{-1}$ in this study), a is the rate constant with the unit of
 25 h^{-1} , $[H_2S]$ is gaseous H_2S concentration in the uptake reactor (ppm), R is the universal gas
 26 constant ($\text{J k}^{-1} \text{mol}^{-1}$), T is the absolute temperature (K), V is the total gas volume in the
 27 reactor (m^3 , 0.000145m^3 in this study), S is the concrete surface exposed to the reactor
 28 atmosphere (m^2 , 0.00905m^2 in this study).

29

$$30 \quad T_{spike} = ([H_2S]_{spike,e} - [H_2S]_{baseline,e}) * 101.325 \text{KPa} * \frac{32 \text{g/mol}}{RT} * V - T_{background} \quad (\text{S2})$$

31 T_{spike} is the mass of H_2S transfer from reactor atmosphere to the concrete coupon over the
 32 experimental period of a specific ‘spike’ test (mg-S), $[H_2S]_{spike,e}$ is the spike H_2S
 33 concentration in the specific ‘spike’ test (ppm), $[H_2S]_{baseline,e}$ is the historical exposure
 34 concentration of H_2S of the coupon (ppm), $T_{background}$ is the mass loss of H_2S due to
 35 background H_2S uptake by the reactor alone (without the concrete coupon) over the specific
 36 ‘spike’ test (mg-S, see the details of calculation in Equation S3).

37

$$38 \quad T_{background} = \sum_{i=1}^n a * ([H_2S]_i + [H_2S]_{i+1}) * 101.325 \text{KPa} * \frac{32 \text{g/mol}}{RT} * V * 0.5 * \Delta t \quad (\text{S3})$$

39 i is i^{th} measurement of gaseous H_2S concentration in uptake reactor in the specific test;
 40 $[\text{H}_2\text{S}]_i$ is the gaseous H_2S concentration in uptake chamber at the i^{th} measurement, n is the
 41 number of measurements of gaseous H_2S concentration over the specific test, Δt is the time
 42 interval between two measurements of H_2S concentration (h).

$$44 \quad T_{\text{baseline}} = \text{SUR}_{\text{baseline}} * S * t = r_{\text{baseline}} * 101.325 \text{KPa} * \frac{32 \text{g/mol}}{RT} * V * t \quad (\text{S4})$$

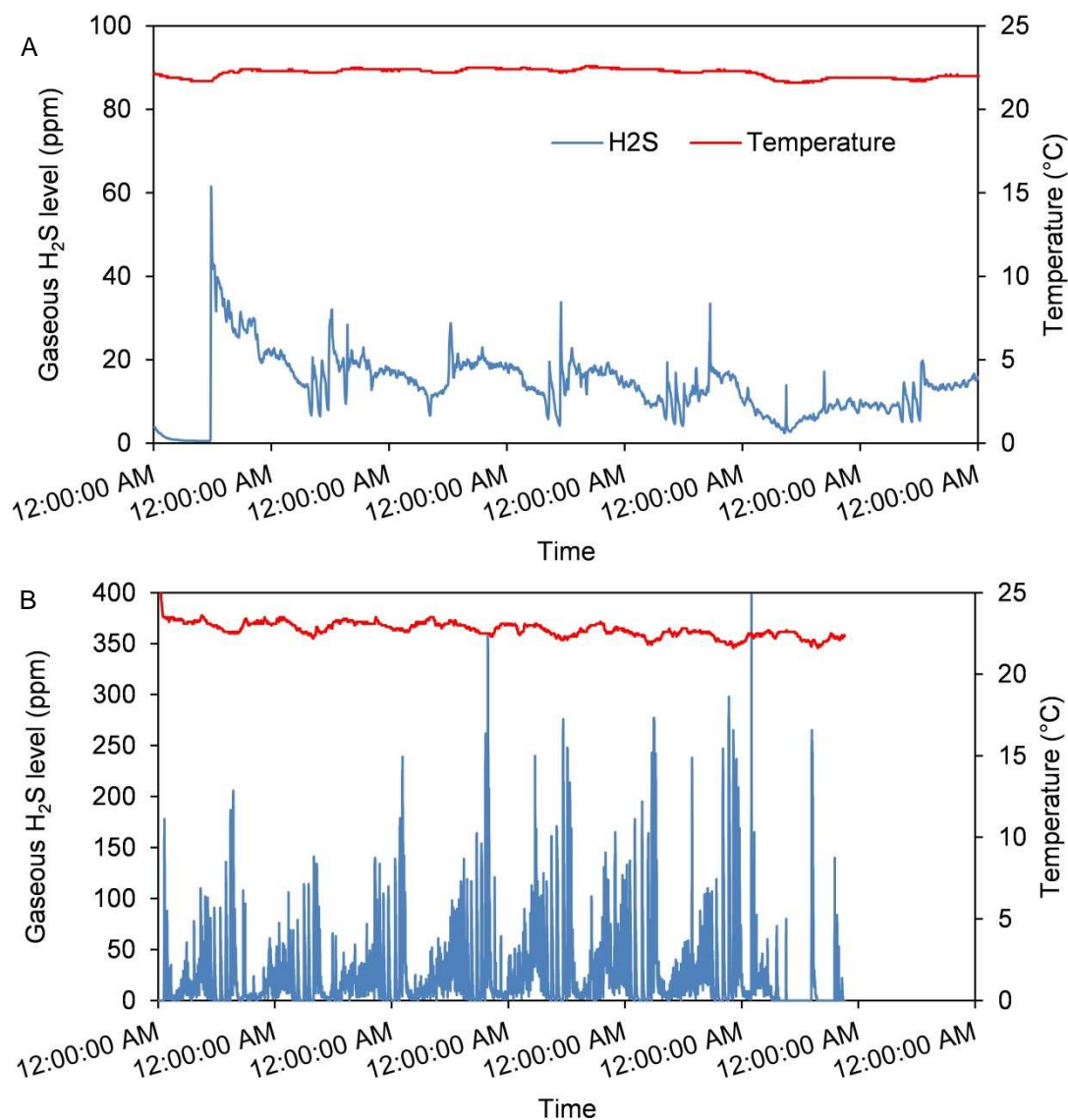
45 where T_{baseline} is the mass of H_2S transfer to the same coupon over the periods equivalent to
 46 that of the specific ‘spike’ test and when exposed to historical H_2S exposure levels (mg-S),
 47 $\text{SUR}_{\text{baseline}}$ is the surface specific SUR of the coupon (background SUR had been deducted
 48 from it) at its baseline H_2S concentration measured in a ‘control’ test ($\text{mg-S m}^{-2} \text{h}^{-1}$), r_{baseline} is
 49 the corresponding H_2S uptake rate of coupon in the unit of ppm h^{-1} , t is the duration of a
 50 ‘spike’ test (h, note here $t = \sum_{i=1}^n \Delta t$).

51

52 **Table S1** Details of H_2S in reactor atmosphere and liquid layer of concrete surface at 15 ppm
 53 and 150 ppm of gaseous H_2S

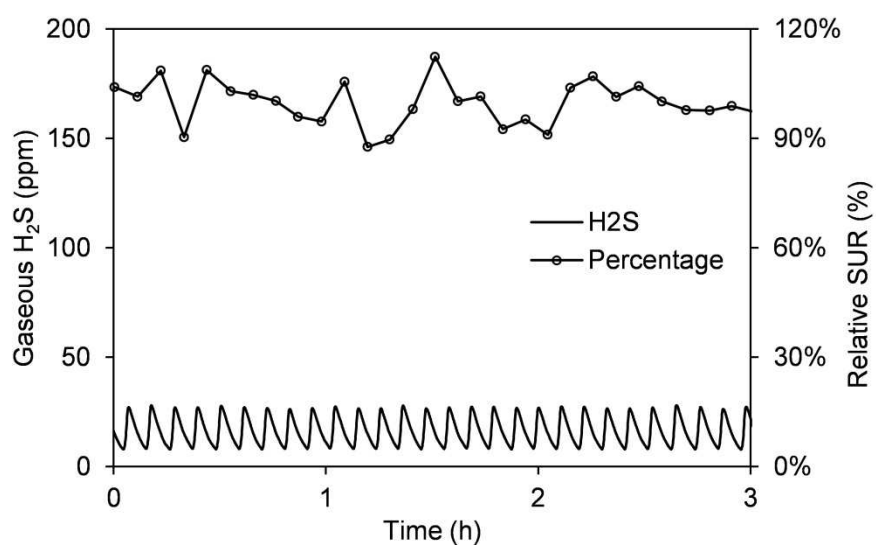
H_2S concentration in atmosphere (ppm)	15	150
H_2S mass in atmosphere (mg-S)	0.029	0.29
H_2S mass in liquid layer H_2S (mg-S)	0.0017	0.017
$(\text{H}_2\text{S}$ mass in atmosphere)/(H_2S mass in liquid layer and atmosphere)	5.5%	5.5%
H_2S concentration in liquid layer (mg-S L^{-1})	0.049	0.49

54 The results in Table S1 are based on the assumption that the concrete coupon has a water
 55 layer of 5 mm and that the H_2S achieves equilibrium in atmosphere and the corrosion layer.



56

57 **Figure S1** – Gaseous H₂S concentrations monitored in a manhole at Melbourne’s Western
58 Trunk Sewer from 5th April 2011 to 11th April 2011 and at Queensland’s Sunshine Coast
59 region from 25th June 2014 to 1st July 2014 is shown in Figure A and B respectively.



60

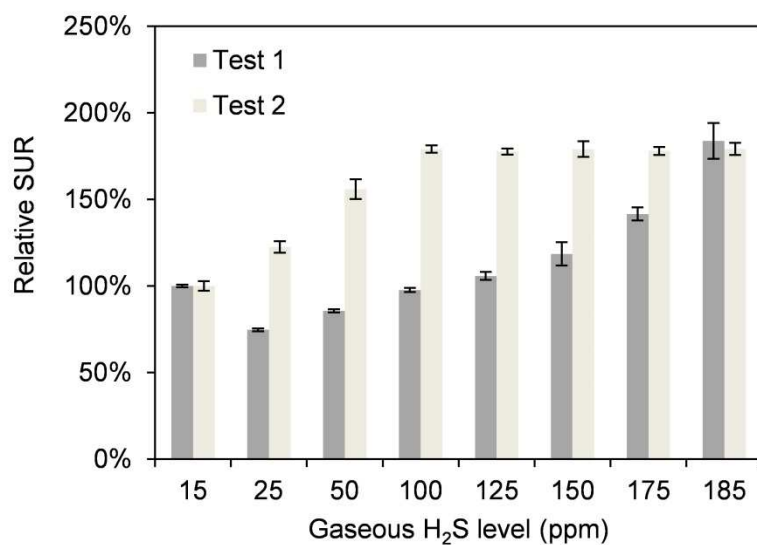
61 **Figure S2** – The temporal H₂S uptake profiles of a coupon (exposure history: 15 ppm H₂S,
62 22-25 °C, 100% relative humidity for 53 months) and the corresponding relative SUR in a
63 control experiment over 3 h.

64

65

66

67



68

69 **Figure S3** – The relative SUR of a coupon previously exposed to 15 ppm for 38 months at
70 various H₂S levels against H₂S concentrations in two independent tests (shown as test 1 and
71 2). Test 1 has a rapid initial increase of H₂S concentration whereas test 2 has a gradual
72 increase of H₂S concentration.